PERGAMON

Journal of Structural Geology 24 (2002) 671–687

JOURNAL OF STRUCTURAL GEOLOGY

www.elsevier.com/locate/jstrugeo

Seismic expression and kinematics of a fault-related fold termination: Rosario structure, Maracaibo Basin, Venezuela

Ted Apotria[a,*], M. Scott Wilkerson[b]

[a]*ExxonMobil Exploration Company, 233 Benmar St., Houston, TX 77060, USA*
[b]*DePauw University, Department of Geology and Geography, 602 S. College Ave., Greencastle, IN 46135, USA*

Received 19 September 2000; revised 26 April 2001; accepted 10 May 2001

Abstract

Fold terminations are primary features of deformed belts and are critical elements in understanding the 3-D kinematics of fault-related folds. Typically, such terminations form due to loss of displacement on the genetically-related thrust fault and/or to along-strike change in fault attitude, forming a lateral or oblique ramp. To unambiguously determine the mechanism responsible for a given fault-related fold termination, footwall cutoffs and along-strike displacement variation must be constrained. Reflection seismic data can provide the detail necessary to uniquely describe these features.

The Rosario structure in the Maracaibo Basin, Venezuela is an example of a natural fault-related fold that possesses a southern termination whose fold/fault geometry and along-strike displacement variation are constrained by industry reflection seismic and well data. We interpret that the fold plunge near the southern termination is due to an along-strike decrease in displacement. The fault geometry associated with the southern termination changes from a flat–ramp–flat at the crest of the structure where displacement is greatest to simply a ramp near the lateral fault tip, without forming a lateral or oblique ramp. We combine these observations regarding displacement and fault geometry with the assumption that along-strike spatial variations reflect temporal variations during development of a fault-related fold to propose a kinematic model for the Rosario structure. Specifically, we suggest that the structure first initiated as an isolated fault ramp within the 'stiff' carbonate and clastic units. With increased shortening, the fault grew to link with upper and lower detachments in the weaker shale units to create a hybridized fault-bend fold. Our model suggests a possible explanation for the evolution of the Rosario structure, and also provides an alternative to existing pseudo-three-dimensional models for fault-related fold growth that relaxes the rigidity in the assumption of along-strike self-similarity.

Keywords: Fold-thrust belts; Fault-related folds; Thrust faults; Fold terminations

1. Introduction

For the last quarter century, structural geologists have attempted to understand the initiation and development of fault-related folds through detailed study of natural examples in fold-thrust belts, by simulation using physical models, and by creation of geometric, kinematic, and mechanical models. Two-dimensional geometric and kinematic modeling, in particular, have experienced significant advances in recent years (see review in Thorbjornsen and Dunne, 1997). These models include:

- fault-bend folds where strata deform over bends in a pre-existing fault (e.g. Suppe 1983),
- fault-propagation folds where strata deform in advance of a growing fault tip (e.g. Suppe and Medwedeff, 1990),
- detachment folds where folds develop above a basal decollement (e.g. Jamison, 1987),
- break-thrust folds where folding precedes development of a through-going fault within the structure (e.g. Fischer et al., 1992), and
- displacement-gradient/fault-arrest folds where folds develop in association with displacement on a fault with a fixed tip line (e.g. Wickham, 1995; Thorbjornsen and Dunne, 1997).

In addition, a more limited number of models explicitly account for variations in the mechanical stratigraphy. In one example, fault ramps nucleate in strong, brittle lithologies and subsequently propagate up and down section to connect with detachments within nearby weaker layers to

* Corresponding author.
E-mail addresses: ted.g.apotria@exxonmobil.com (T. Apotria), mswilke@depauw.edu (M.S. Wilkerson).

0191-8141/02/$ - see front matter
PII: S0191-8141(01)00123-7

form fault-bend folds (e.g. Eisenstadt and DePaor, 1987). This significantly differs from previous fault-bend fold models in which the ramp–flat fault geometry becomes established before substantial displacement occurs and flexural slip is assumed throughout the section (e.g. Suppe, 1983).

Several workers have explored the implications of extending these two-dimensional geometric models into the third dimension (e.g. Wilkerson et al., 1991; Fischer and Woodward, 1992; Shaw et al., 1994; Fischer and Wilkerson, 2000; Rowan and Linares, 2000; Wilkerson et al., 2002). Generally speaking, one of two approaches is used:

1. 3-D models are created by systematically varying fault slip and/or fault geometry on adjacent serial sections (e.g. Wilkerson et al., 1991; Shaw et al., 1994; Fischer and Wilkerson, 2000; Rowan and Linares, 2000; Wilkerson et al., 2002). An example might be a fault-bend fold with zero slip at one end and finite slip at the crest.
2. 3-D models are created from adjacent serial sections that may have experienced different deformation mechanisms resulting in a composite fold style along the strike length of the fold (e.g. Fischer and Woodward, 1992). An example might be a fault-bend fold in the center of the structure that changes to a fault-propagation fold at the termination.

Both modeling approaches likely are reflected in natural structures and have their merits in enhancing our understanding of the lateral development of fault-related folds. Much insight, however, is still to be gained by careful study of natural structures in light of these modeling efforts. In particular, comparison of natural fault-related fold terminations with the central portion of the same folds may provide clues as to how such structures laterally developed.

Fault-related fold terminations account for much of the 3-D variability observed in fold-thrust belts around the world. Specifically, fault-related folds laterally extend with relatively constant geometry for kilometers and then abruptly plunge to form a termination. These plunging terminations not only are critical elements in analyses of the 3-D geometry and kinematics of fault-related folds, but when located in the subsurface, are key features that help create the 3-way and 4-way closure necessary to trap hydrocarbons. Formation of most contractional fault-related fold terminations is controlled by variations in fault slip, variations in fault attitude (e.g. an oblique/lateral ramp), or some combination of the two (Wilkerson et al., 2002). Wilkerson et al. (2002) show that discerning the relative contributions of these mechanisms in causing a fault-related fold to terminate based solely on its geologic map expression can be ambiguous. For example, the map pattern of along-strike changes in stratigraphic separation along a fault may be produced by (a) a displacement gradient, (b) a change in fault geometry (an oblique/lateral ramp), (c) erosion, and/or (d) tilting. Likewise, a single cross section provides one measure of fault attitude and fault displacement, but cannot define the 3-D variation required to interpret the termination mechanism. Rowan and Linares (2000) attempted to address this issue by using fold axial-surface maps based on serial 2-D reflection seismic lines to define the underlying fault structure. They demonstrated that changes in fault attitude, displacement magnitude, and stratigraphic position of detachments actually lead to non-unique interpretations for axial-surface maps of fault-related fold terminations without good seismic control.

Therefore, to unambiguously determine the underlying cause for a fault-related fold termination, footwall cutoffs and displacement variation must be constrained. Serial profiles based on good quality seismic data can provide the necessary geometrical constraints and may permit inference of the lateral development of the fold if one can assume that spatial variations along strike are related to temporal variations during development of the structure.

We provide a natural example of a fault-related fold, the Rosario structure in the Maracaibo Basin, Venezuela that possesses a reasonably simple, well-constrained southern termination in which industry reflection seismic and well data help define the fold/fault geometry and displacement distribution. In addition to determining the mechanism(s) responsible for causing this termination, we use our interpretation as a basis for proposing an alternative model for the lateral evolution of the Rosario structure and similar fault-related folds.

2. Case Study: Rosario Structure, Venezuela

The Rosario structure is a contractional fault-related fold located in the western Maracaibo Basin of Venezuela. Regionally, it is bounded on the west by the Sierra de Perija mountains, on the east by Lake Maracaibo, and on the southeast by the Merida Andes (Fig. 1). More locally, a smaller fault-related fold complicates the Rosario structure to its immediate east (referred to as Rosario East; Fig. 1). The Rosario oil field was discovered in 1954 in association with the Rosario structure and has an estimated ultimate recovery of about 50 million bbls of oil, with production from fractured Cretaceous carbonates and Eocene fluvial clastic reservoirs (Molina, 1992).

2.1. Stratigraphy and tectonic history

A general stratigraphic column (Fig. 2) for the western Maracaibo Basin illustrates formations and stratigraphic thicknesses from the CR-12 well at Rosario field. The column also qualitatively depicts the mechanical stratigraphy, including the inferred location of detachment horizons.

Three major tectono–stratigraphic successions define the tectonic environment and the mechanical units of the strati-

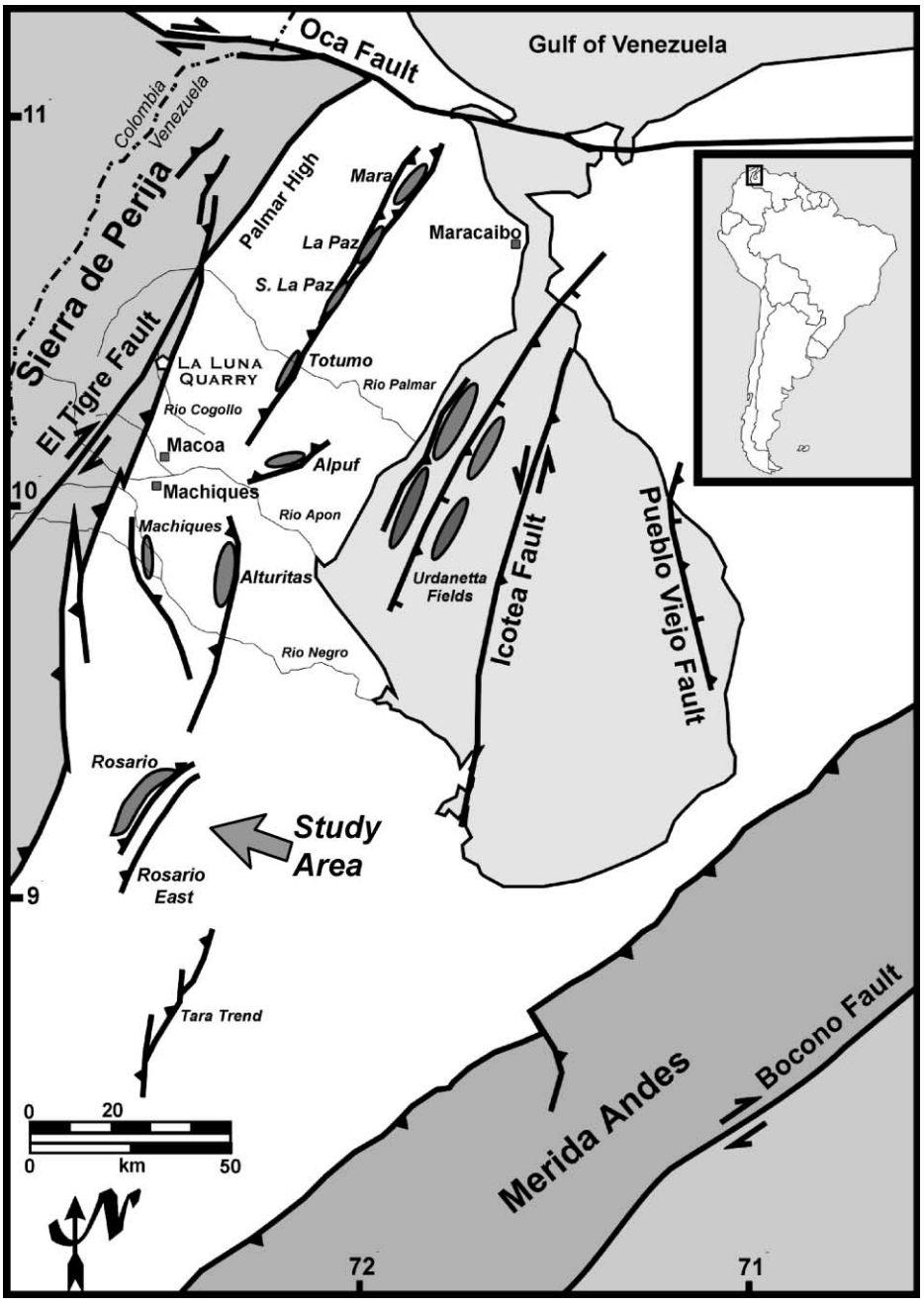

Fig. 1. Location map showing principal structural features of the western Maracaibo Basin, Venezuela. Gray polygons denote selected oil fields. The La Luna quarry is located along the Perija frontal monocline and exposes an outcrop analog for some fault-related folds in the western Maracaibo Basin (see Fig. 6).

graphic section: a rift-related succession, an open-marine foredeep section, and a clastic continental margin sequence (Kellogg, 1984; Roure et al., 1997). The rift-related deposits formed during the Jurassic–Early Cretaceous as rifting and volcanism related to the opening of Western Tethys produced a NE–SW-trending graben system along the present-day Perija Mountains that extended into the Maracaibo Basin. This graben system was filled with continental red beds of the La Quinta Formation (Maze, 1984). These red beds were subsequently overlain by post-rift, passive margin deposits including the Cretaceous Rio Negro sandstones, and the Cretaceous Cogollo Group carbonates (Apon, Aguardiente, and Maraca Formations). These units are relatively competent intervals based on outcrop studies and well data and comprise part of the 'stiff layer' for structures in the basin (DeToni and Kellogg, 1993; Roure et al., 1997; Fig. 2).

During the Late Cretaceous to Paleocene time, the margin transformed to an open marine environment dominated by foredeep deposits of the La Luna limestone (a world-class oil-generating source rock in the Maracaibo Basin; Hedberg, 1931), Colon Shale and Mito Juan Formation.

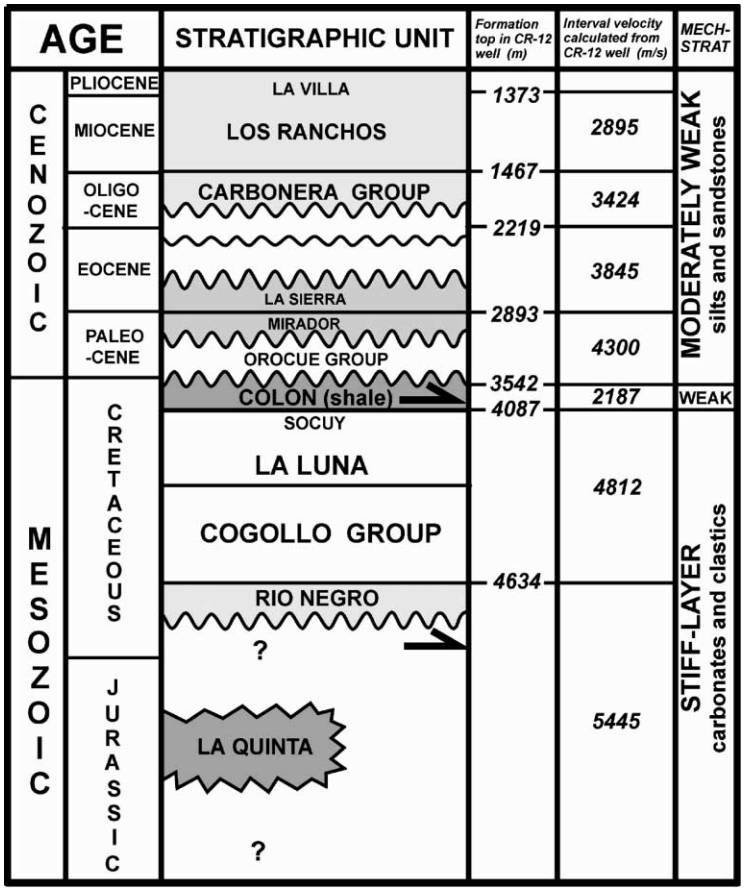

Fig. 2. Generalized stratigraphy of the western Maracaibo Basin. Formation tops in depth (meters below a 33 m KB) and interval velocities used for depth conversion are posted from the CR-12 well. Formation top indicated as Miocene is a Mid-Miocene seismic reflector. Qualitative mechanical stratigraphy and the location of inferred detachments are also depicted. The La Luna Formation is part of an overall stiff carbonate section, but is thin-bedded and is relatively weak compared with the underlying Cogollo Group carbonates (e.g. Fig. 6).

Convergence of the Caribbean plate produced contraction and uplift in the Perija Mountains and Maracaibo Basin and local inversion of the former graben system. This deformation was marked by unconformities in the Mid-Eocene (43 mybp) and Late Eocene (39 mybp; Fig. 2), and is contemporaneous with the Cordilleran Orogeny in Colombia (Kellogg, 1984).

Subsequently, a Mid-Miocene and younger Andean Orogeny imposed widespread contractional deformation of the Maracaibo Basin, producing a stratigraphic succession of alternating shales, silts and sandstones. During this contraction, older rift-related faults experienced oblique-slip reactivation (e.g. the Urdanetta fields, the Boscan fields, and the N–S-trending Icotea and Pueblo Viejo faults in Lake Maracaibo; Fig. 1; Roure et al., 1997).

Seismic data suggest that the magnitude of shortening in the western Maracaibo Basin is greatest in the Perija Mountains and decreases east towards Lake Maracaibo. In the Perija Mountains, duplex structures involving the Jurassic–Cretaceous strata are interpreted to have several kilometers of cumulative displacement (DeToni and Kellogg, 1993), whereas subsurface structures to the east (e.g. Rosario, Alturitas, and Alpuf fields) have faults with displacement of less than 2 km (Molina, 1992; Roure et al., 1997).

2.2. Seismic control and data quality

Interpretation of the Rosario structure is constrained by nine, 2-D time-migrated seismic lines (1985- and 1990-vintage, Fig. 3a–i from north to south). Interval velocities calculated from seismic well ties from the CR-12 well (Fig. 2) were used to constrain a vertical, 2-D depth conversion implemented in Geosec^{TM} restoration software. This depth-converted 2-D interpretation was then transformed into a 3-D model of faults and horizons using 3DMove^{TM} that yielded subsurface depth-structure maps on the tops of the La Luna Formation (Fig. 4) and the Colon Shale (Fig. 5). These maps are also constrained by the CR-09 and CR-12 wells that penetrate the top of the Cretaceous section (Fig. 4).

Seismic data quality for the Rosario structure is highly variable (Fig. 3). The uppermost parts of the seismic sections (generally above 3 s) contain fairly high-quality data. The Paleocene and younger sections in this interval consist of alternating packages of sands, silts, and shales and

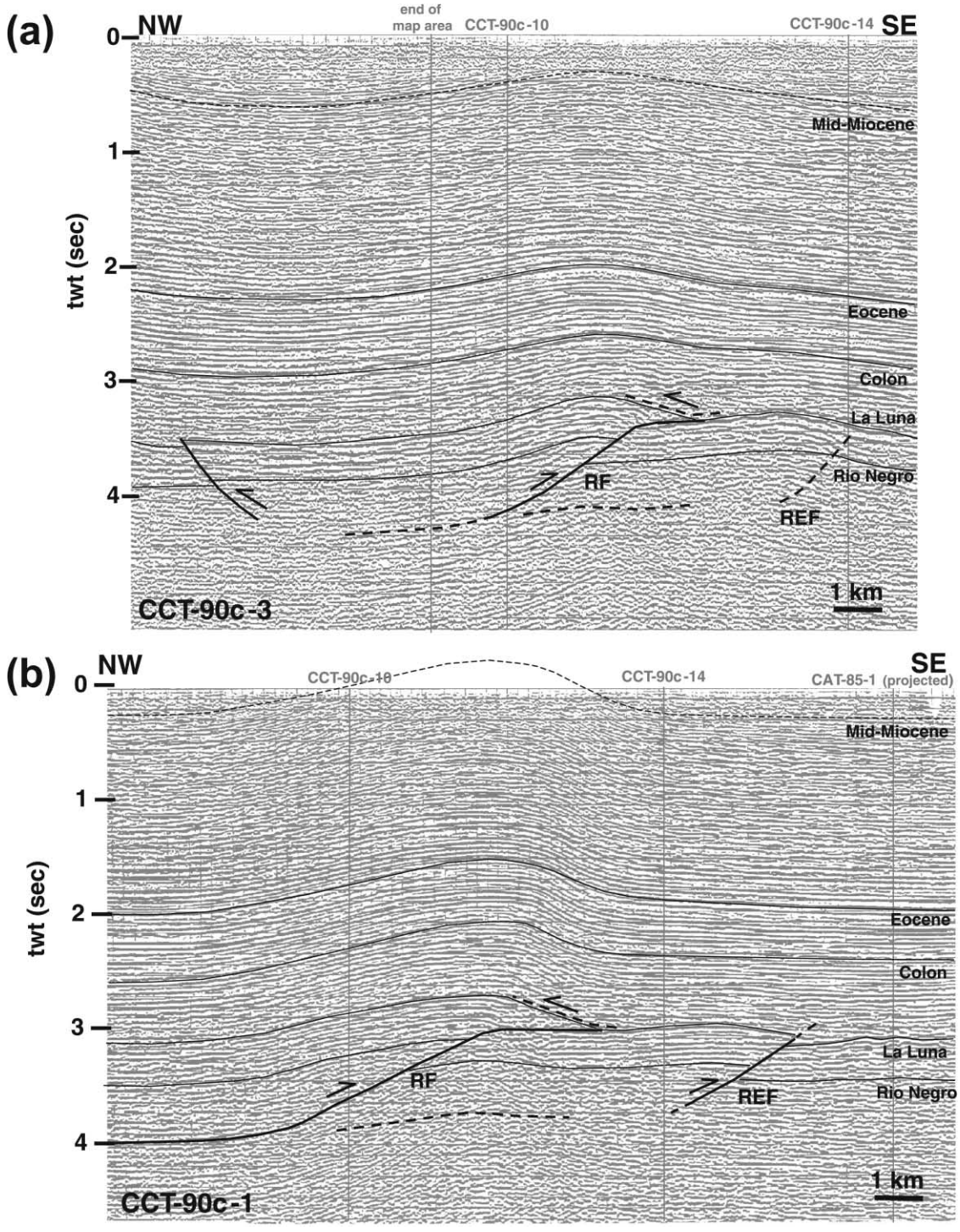

Fig. 3. Two-dimensional, time-migrated seismic lines over the Rosario structure (seismic line locations shown on Figs. 4, 5 and 7). The seismic lines are 1985- and 1990-vintage, and vertically exaggerated from depth approximately 2:1 at the level of top La Luna Formation. Formation tops are labeled on the right, the approximate position of the Mid-Miocene surface is dashed, RF = Rosario Fault, and REF = Rosario East Fault. Tie line locations are labeled in gray. Seismic lines with duplicated carbonate section exhibit velocity pull-up below the thrust fault (dashed lines below Rio Negro). (a) CCT 90c-3, (b) CCT 90c-1, (c) CCT-90c-10 (profile is oblique to both the dip and strike directions of the fold), (d) CCT-90-c-14 (crest), (e) CAT-85-1, (f) CAT-85-2, (g) CAT-85-3, (h) CAT-85-4, (i) CAT-85-5 (near the Rosario southern termination).

simply reflect folding from the deeper structures, without being faulted at the seismic scale. The underlying Colon Shale also is unfaulted and has a low-amplitude, semi-continuous reflection character (e.g. Fig. 3e). It normally has a thickness of about 550 m, but can exhibit local thickness variations, particularly where faults emerge from the underlying carbonate section. Seismic interpretation of the faulted section relies on two high-impedance and

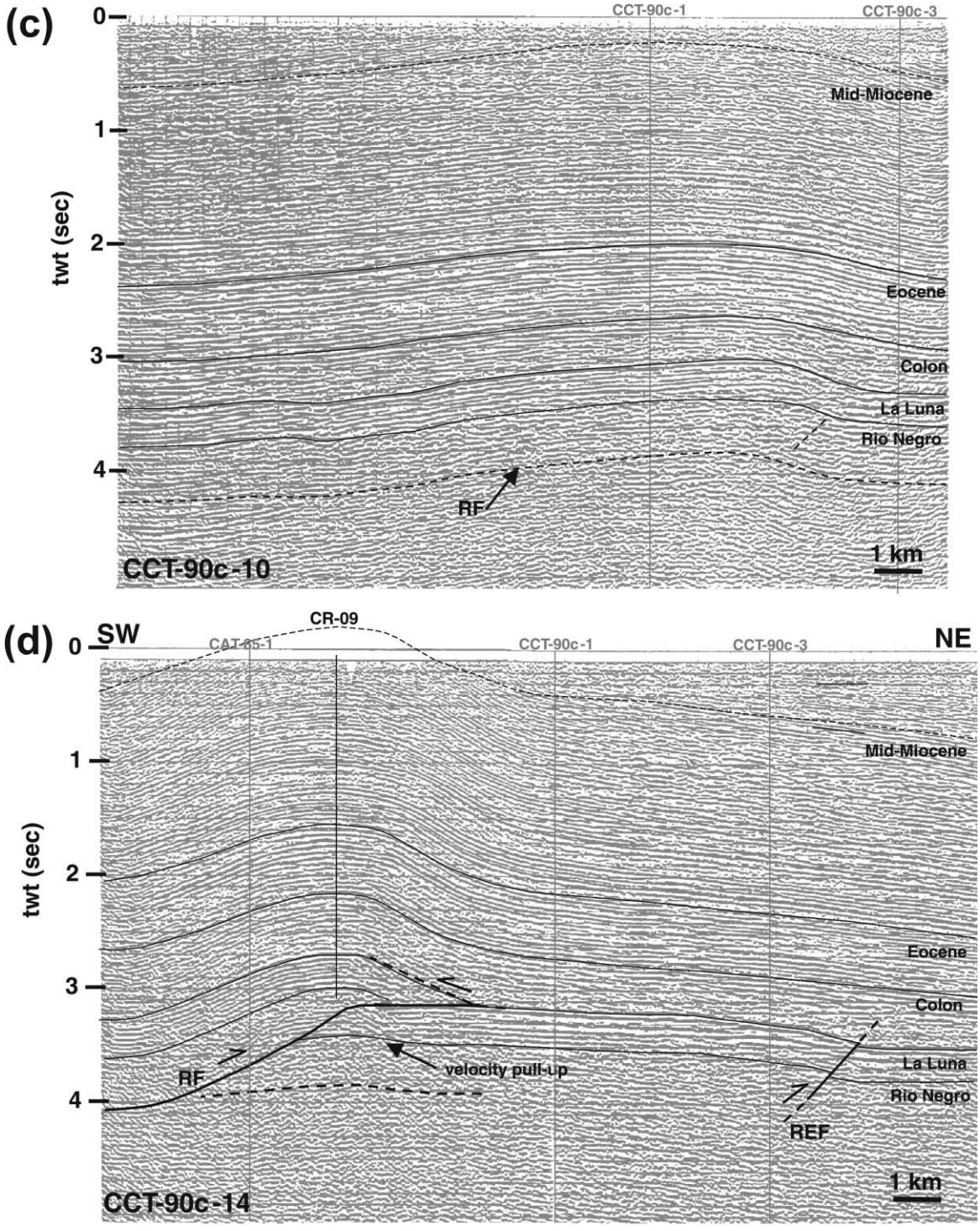

Fig. 3. (*continued*)

continuous reflections that mark the top and bottom of the carbonate section and that tie to the CR-12 well (Fig. 3). The first reflection occurs between the Colon Shale and the top of the carbonate section (Socuy and La Luna Formation; hereafter referred to as the La Luna Formation); this lithologic change also marks the mechanical transition from the stiff unit (below) to a weak clastic unit (above). A second strong impedance contrast occurs at the base of this carbonate section and the top of the underlying Rio Negro clastic section. These two strong reflections bound a total carbonate section that is about 547 m thick in the CR-12 well. Offset on faults within the carbonates is well-imaged near the Colon Shale–La Luna Formation contact, but becomes more poorly imaged within the Rio Negro and deeper section. Only those faults that offset the La Luna or that produce a fold have been interpreted on the seismic data

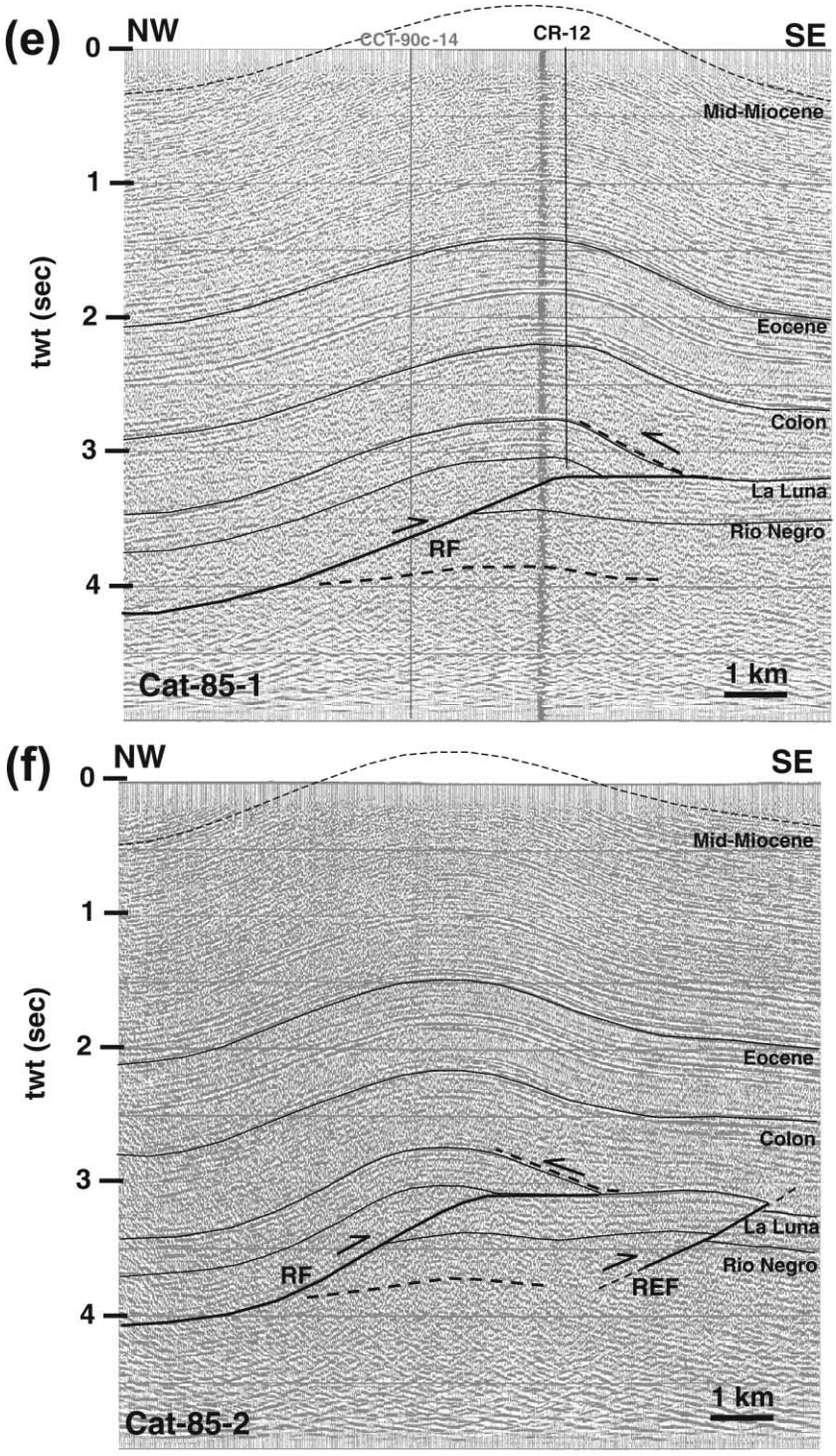

Fig. 3. (*continued*)

(Fig. 3). The data quality becomes relatively poor beneath the Rio Negro section.

2.3. Seismic interpretation

As is often the case with structures constrained by 2-D seismic lines, interpretation of the Rosario structure was data driven, but model guided. We honored the seismic data where possible, and where confronted with areas of poor seismic quality, we completed our interpretations such that they were geometrically admissible and consistent along strike.

Many of the fundamental features of the Rosario structure are best imaged at the crest of the fold, which is crossed by

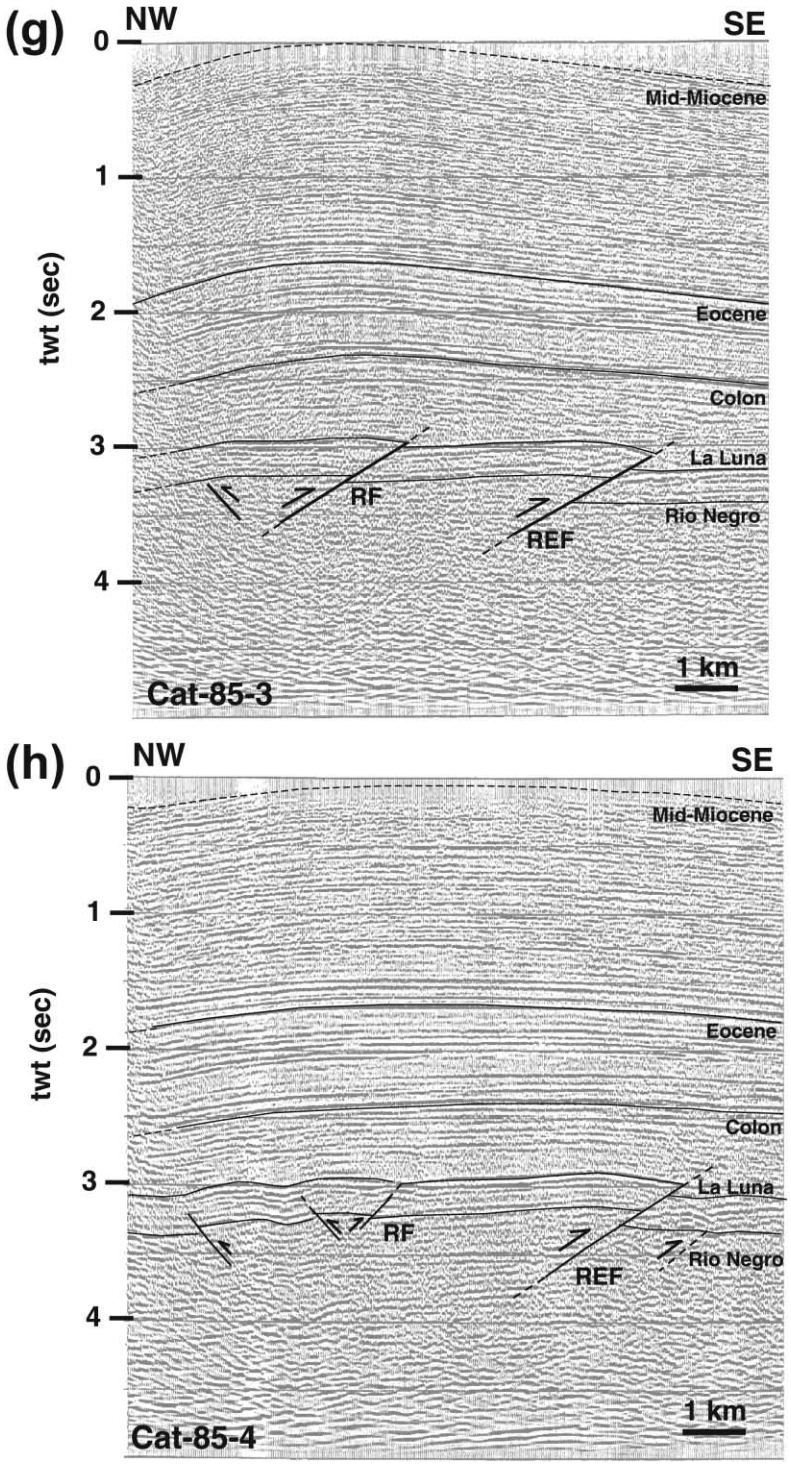

Fig. 3. (*continued*)

seismic line CCT-90c-14 (Fig. 3d). On this line, the fault exhibits a flat–ramp–flat geometry that creates a fault-bend fold in its hanging wall. Specifically, La Luna and Rio Negro strata are truncated by the fault and are displaced onto a footwall flat near the La Luna/Colon contact. Their forelimb dips are slightly greater than those on the backlimb, defining a weak asymmetry toward the east. The exact positions of the La Luna and Rio Negro footwall cutoffs are not well-imaged and are obscured by velocity pull-up beneath the hanging-wall carbonates (Fig. 3d). However, we estimate that displacement onto the upper flat is approximately 2 km on this section (the maximum displacement along the length of the entire structure). Examination of line lengths between Cretaceous carbonates and Tertiary

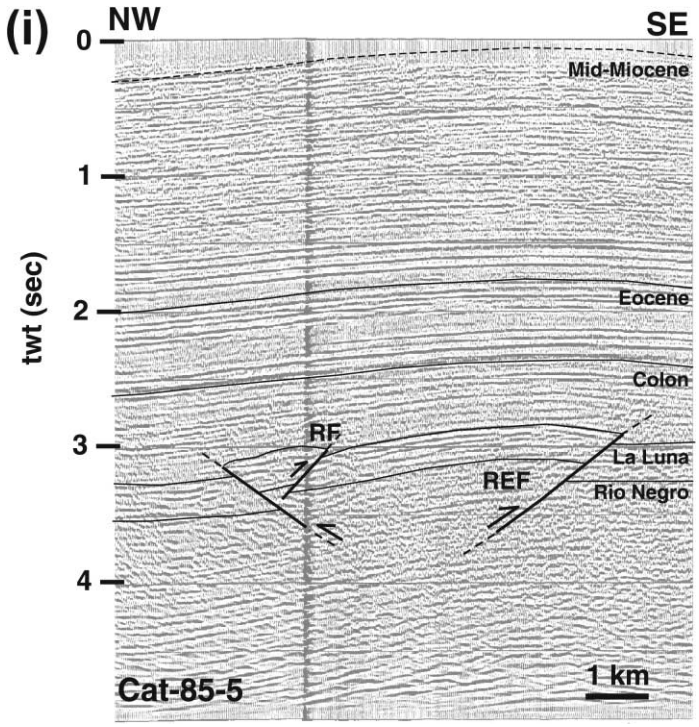

Fig. 3. (*continued*)

clastics suggests an imbalance of shortening at the seismic scale (e.g. Fig. 3d). Seismic data in the vicinity of Rosario suggest the shortening of the Tertiary is not transferred into the foreland (e.g. Fig. 3d). Instead, we suggest shortening is accommodated by a wedge structure that transfers displacement back towards the hinterland, similar to nearby outcrop analogs (Fig. 6). Lastly, timing of deformation at Rosario is constrained to have begun in the Mid-Miocene based on growth strata in the highest parts of the section (e.g. Fig. 3d). Based on present-day topographic relief, the structure remained active into Pleistocene and Recent times as well.

To the north of line CCT-90c-14 (Fig. 3d), the overall geometry of the Rosario structure remains similar (Fig. 3a and b). Although the seismic data do not extend to the extreme northern termination of the structure, interpretation of the seismic data suggests that the fault loses displacement to the north and that the forelimb dips more shallowly along-strike toward the north. In addition, the Rosario fold hinge changes trend toward the north as well. This change in trend is shown particularly well by tracing the zero-dip contour (blue) on the La Luna and Colon dip maps (Figs. 4b and 5b; dashed lines are fold hinge). A structure-contour map on the Rosario thrust fault also reflects this change in fault ramp strike from N10°E in the center of the structure to N65°E at its northern end (Fig. 7). The northern portion of the ramp is oblique to the assumed regional transport direction of 130°, which is approximately perpendicular to the Perija Mountain front (Fig. 7).

To the south of line CCT-90c-14 (Fig. 3d), significant differences in the overall geometry of the Rosario structure exist relative to the crest. Over a distance of about 4 km, the fold loses distinguishing elements such as a well-developed backlimb and a hanging-wall ramp on footwall flat (compare Fig. 3d–f with Fig. 3g). Correspondingly, the Rosario fault also changes from a flat–ramp–flat geometry to simply a ramp. Although a lower flat may accommodate the shortening observed near the ramp, there is no direct evidence for it based on fold shape. Measured offset of the La Luna Formation also decreases from about 2 km at the crest (Fig. 3d), to 1.5 km on line CAT-85-1 (Fig. 3e), to 1 km on line CAT-85-2 (Fig. 3f), to about 100 m on line CAT-85-3 (Fig. 3g). This loss of 1.9 km of displacement over a distance of about 8 km is equivalent to a differential displacement shear angle of $\tan^{-1}(1.9/8) = 13°$; a substantial amount, but well within the range of documented displacement gradients elsewhere (Wilkerson, 1992). We suggest this loss of displacement on the Rosario structure is primarily accommodated by displacement transfer to the Rosario East fault (Fig. 4a), which gains displacement over this same interval. This is evident from the top La Luna structure map as two discrete en échelon anticlines separated by the Rosario fault (Fig. 4a, two dashed lines). The Colon Shale dampens the interaction of the two thrust faults in the shallower Tertiary section. The relay between the two folds is evident as a single fold hinge that changes trend in the transfer zone (Fig. 5a, single dashed line).

3. Discussion

The Rosario case study sheds insight on two processes

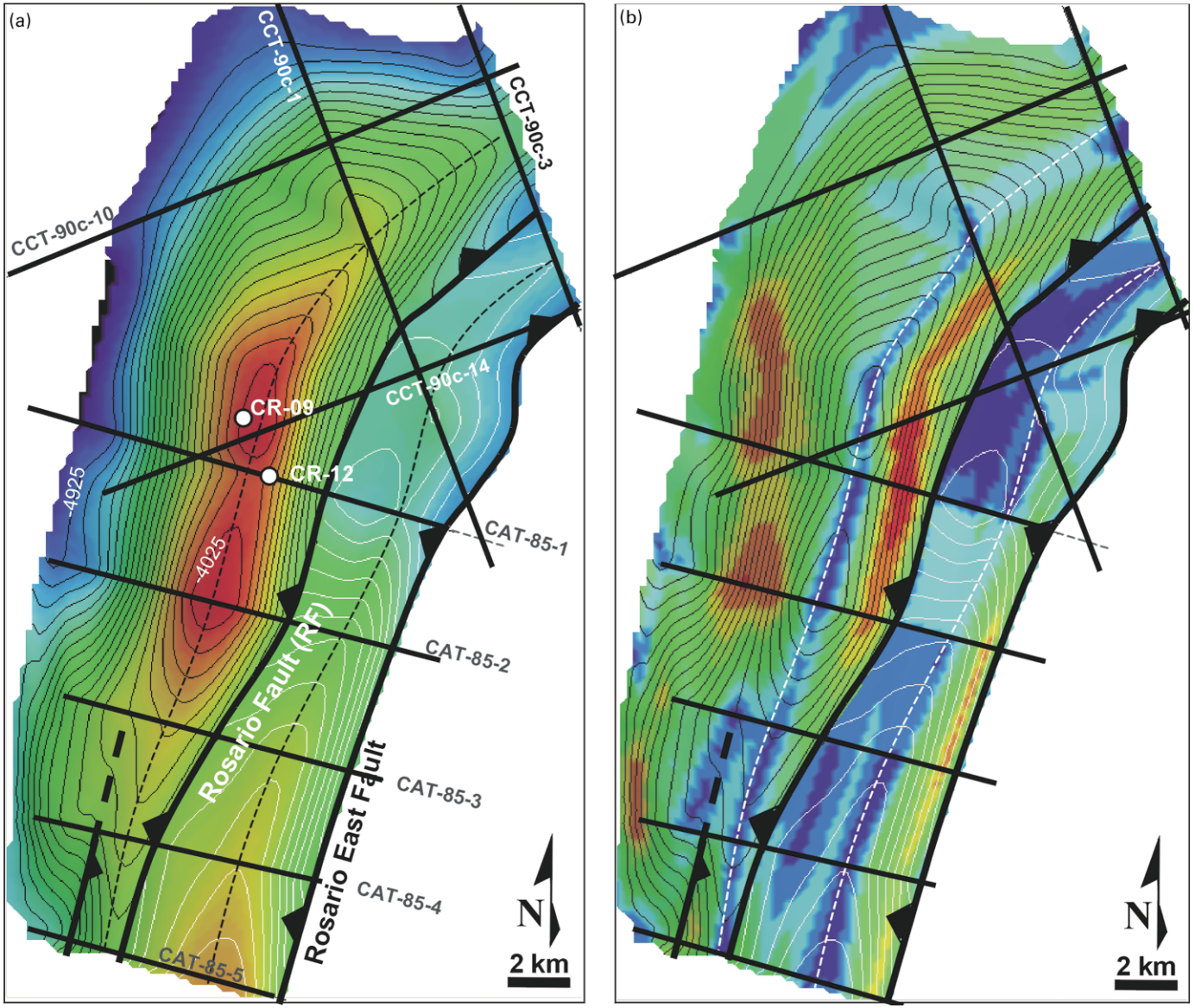

Fig. 4. Top La Luna Formation (a) sub-sea depth structure and (b) dip magnitude maps. Solid lines represent positions of seismic lines, whereas dashed lines represent fold hinges for the Rosario and Rosario East structures, respectively. (a) Contour depths range from −4925 m (blue) to −4025 m (red) with a contour interval of 50 m. The location of wells that penetrate the top Cretaceous carbonates are also posted. (b) The dip map has a maximum value of 22° (red) and a minimum value of 0° (blue).

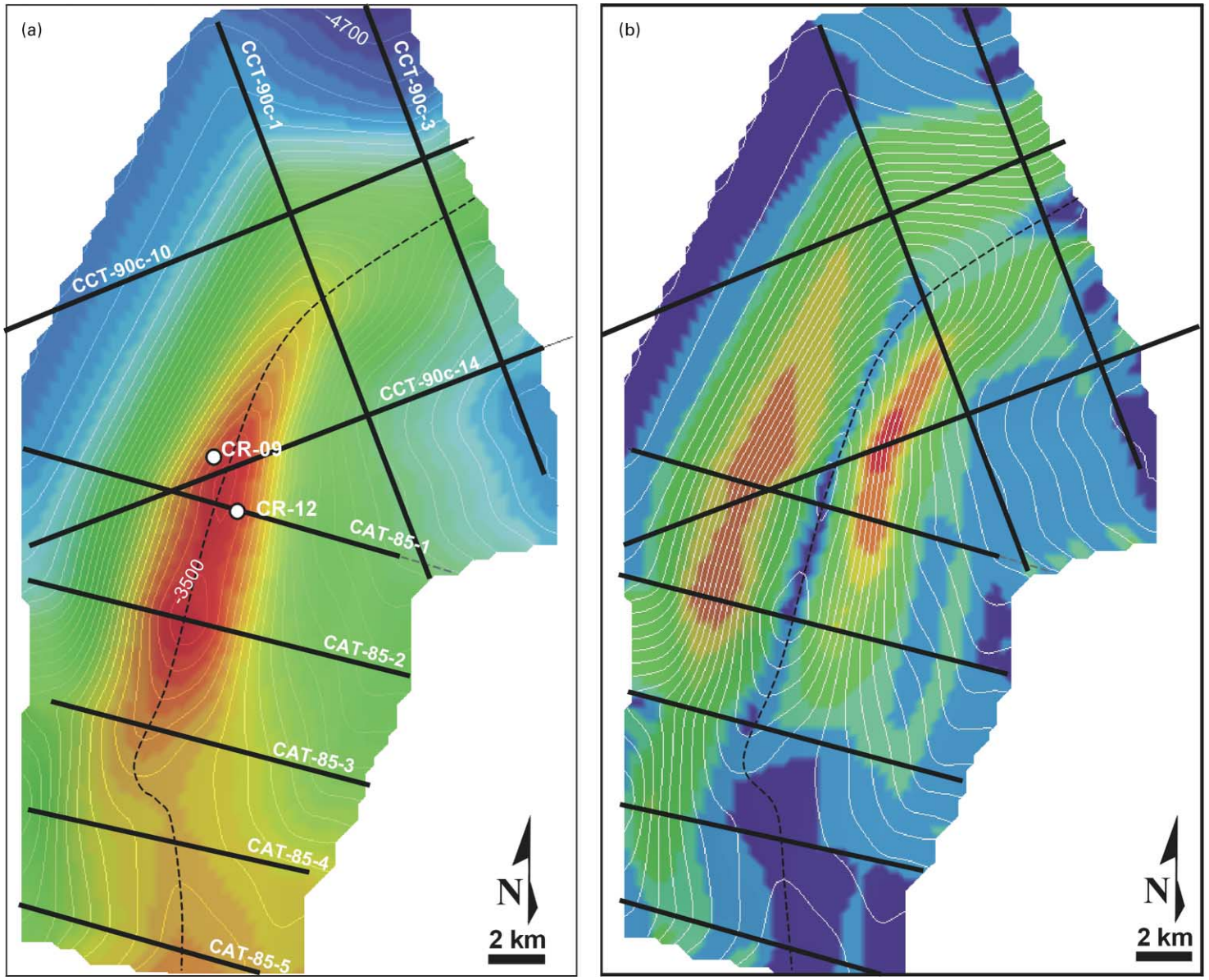

Fig. 5. Top Colon Shale (a) sub-sea depth structure and (b) dip magnitude maps. Solid lines represent positions of seismic lines, whereas the dashed line represents a single fold hinge at the Colon level for the combined Rosario and Rosario East structures. (a) Contour depths range from −4700 m (blue) to −3500 m (red) with a contour interval of 50 m. (b) The dip map has a maximum value of 18° (red) and a minimum value of 0° (blue).

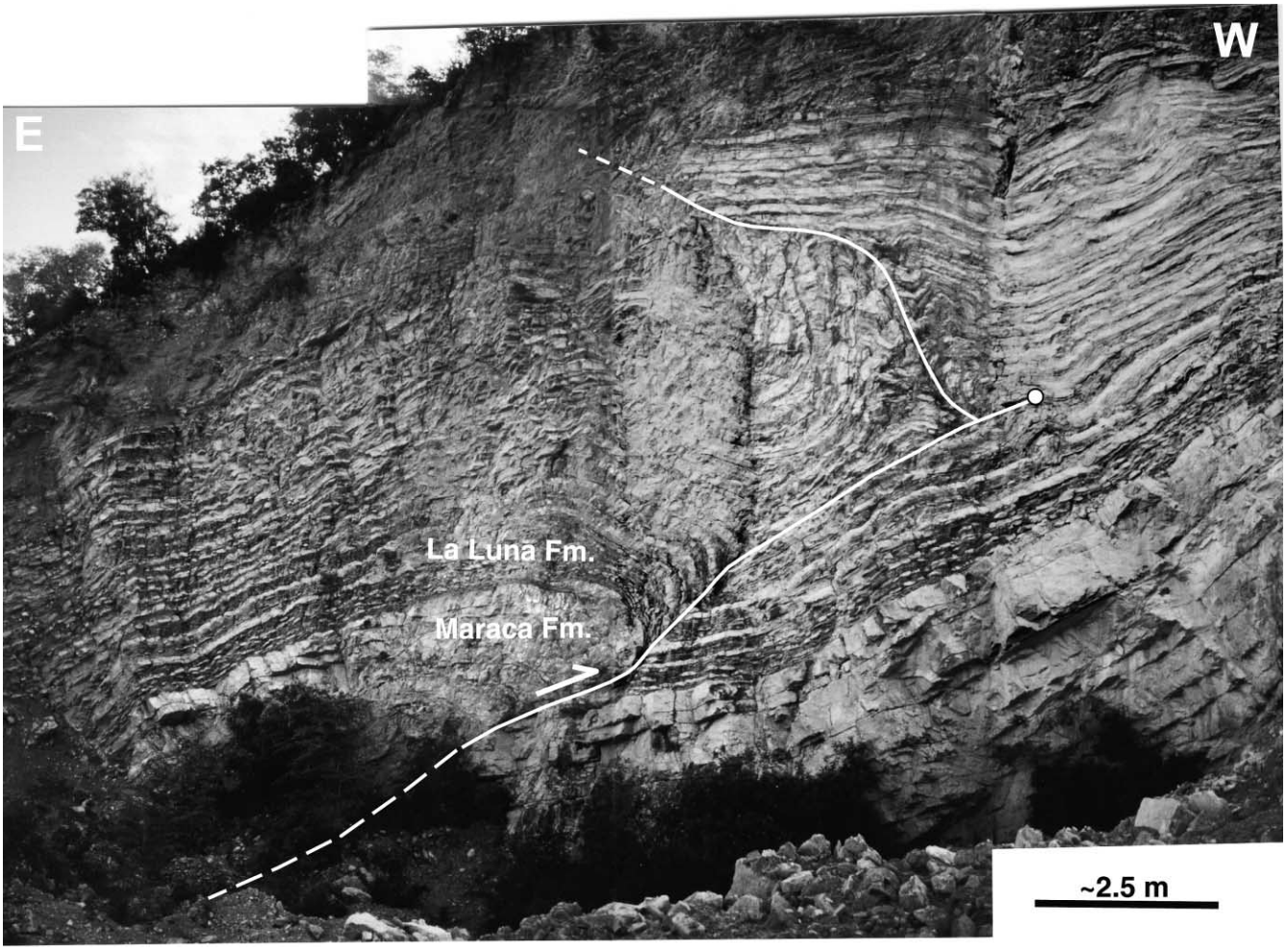

Fig. 6. Outcrop analog from the La Luna quarry that resembles several seismically-imaged, fault-related folds in the western Maracaibo Basin (see Fig. 1 for location). The lower massive unit in the photo is the Maraca Formation of the Cogollo Group carbonates, which is overlain by the thin-bedded, La Luna Formation. The deformation style and thickening that occurs at outcrop scale where the fault emerges from the massive, 'stiff' unit is similar to that seen at seismic scale where faults emerge from the 'stiff' carbonate and clastic section into the 'weak' Colon Shale. View is to the south.

active at its southern termination: the mechanism that causes the structure to terminate, and the development and lateral propagation of the structure.

With regard to the mechanism causing the southern termination of the structure, Wilkerson et al. (2002) show that without cutoff information to constrain variations in fault geometry and fault displacement, the inference of the mechanism causing a fault-related fold to terminate can be ambiguous. Interpreted cutoffs based on seismic data over the Rosario structure (Fig. 3d–i) do provide these constraints and demonstrate that the southern termination is produced by a loss of displacement to the south and not due to formation of a lateral/oblique ramp (see Fig. 7). Moreover, the loss of displacement apparently is accommodated by transfer of displacement to the Rosario East structure (Fig. 3d–i) and other smaller faults with both east and west vergence farther to the south. The oblique ramp observed in the northern part of the study area does not relate to formation of the southern termination, and may or may not influence creation of the northern termination beyond the extent of our seismic data. For our analysis, we only can conclusively determine that it produces a significant change in trend in Rosario's fold axis and cannot relate it to formation of any fold termination.

The change in character of the Rosario structure from its crest to its southern termination may provide insight into how the feature developed. To interpret this development, one must first address how features at fault tips relate to structures in more central portions of the fault-related fold. Wilkerson et al. (2002) provide three models for the lateral development of contractional fault-related folds:

1. structures began as small features that propagated laterally from the center as displacement increased on the underlying fault,
2. structures began as large, laterally continuous features with their dimensions set from the onset of deformation, or
3. structures result from the coalescence of many small faults that eventually linked to form a common fault surface.

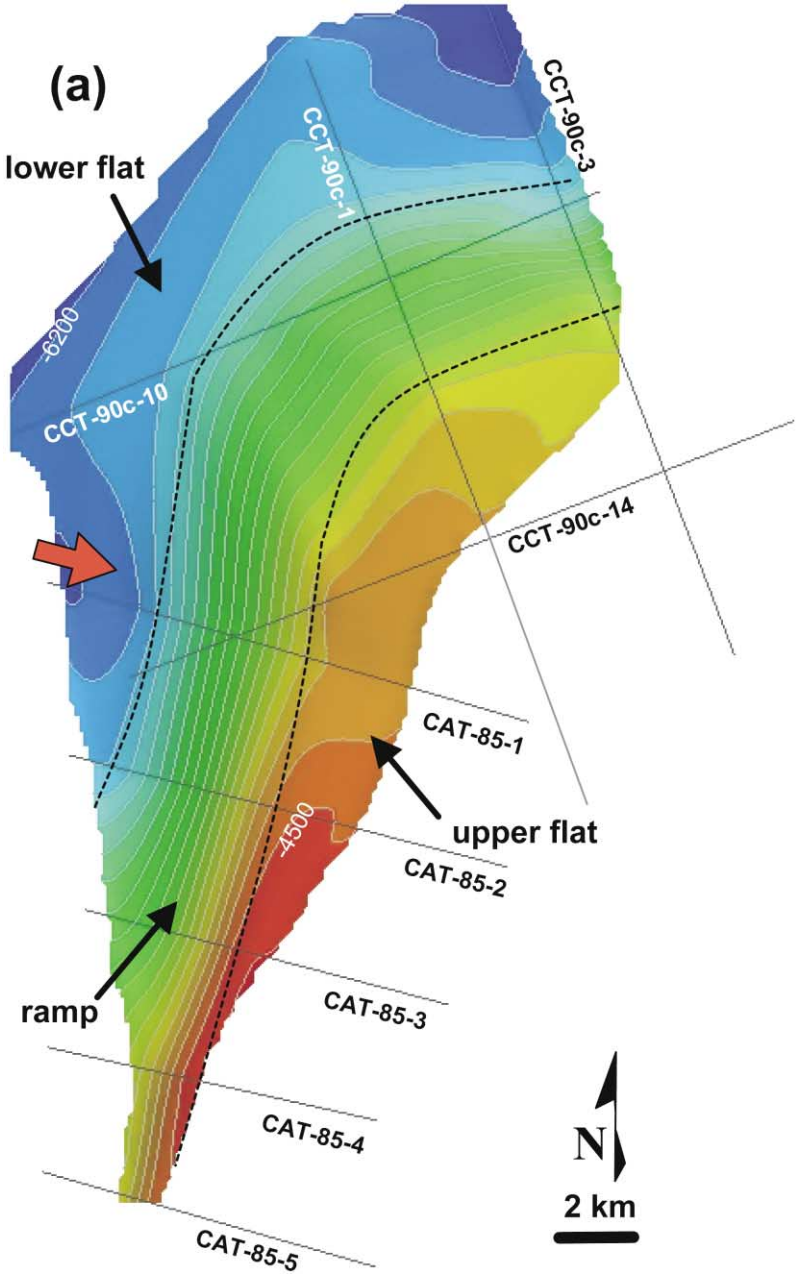

Fig. 7. Depth structure-contour map of the Rosario Fault. Contour depths range from −6200 m (blue) to −4500 m (red) with a contour interval of 100 m. The red arrow shows the assumed regional transport direction approximately perpendicular to the Perija Mountain Front (see Fig. 1). Dashed lines represent approximate boundaries between the ramp and the two flats; observe that no lower flat is interpreted south of seismic line CAT-85-2 (Fig. 3f).

Although we do not have the strain data necessary to discern between these three models for the Rosario structure, we can suggest a potential kinematic model, if we are allowed to assume that structures at the termination mimic earlier stages of more central parts of the structure.

3.1. Trading space for time: redefining the self-similar approach

As mentioned previously, there are two general approaches for describing the along-strike 3-D geometry of fault-related folds:

1. systematically varying fault slip and/or fault geometry on adjacent serial cross sections while maintaining the same fault-related folding mechanism (e.g. Wilkerson et al., 1991; Shaw et al., 1994; Fischer and Wilkerson, 2000; Rowan and Linares, 2000; Wilkerson et al., 2002), or
2. using individual serial cross sections that have independently experienced different folding styles, but

which have eventually merged to create a composite fault-related fold (e.g. Fischer and Woodward, 1992).

Combining these two approaches with the three models of lateral development of fault-related folds (Wilkerson et al., 2002) lead to a variety of kinematic interpretations for a given structure. Probably the most straightforward interpretation is that of *self-similar* propagation of a fault-related fold.

Fischer and Woodward (1992) define self-similar propagation based on the premise that displacement along a fault is proportional to the duration of thrusting and that other characteristics of the structure (e.g. fault dip, folding style, etc.) are held constant along strike. Thus, in simple fold-thrust structures, one might infer that structures near thrust tips represent the earliest stages of deformation and those near the crest represent the latest stages (i.e. effectively trading observed spatial variation for temporal variation). Fischer and Woodward (1992) questioned the usefulness of this technique based on two field studies that suggested more complicated kinematics. Wilkerson et al. (1991) created *pseudo-three-dimensional* models of idealized fault-related folds (e.g. Suppe, 1983; Suppe and Medwedeff, 1990). They effectively broadened the definition of the self-similarity by varying displacement and/or fault geometry along strike in order to produce measurable changes in the overlying fold geometry. The pseudo-three-dimensional approach also has been used to study other types of natural and idealized fault-related folds (e.g. Shaw et al., 1994; Fischer and Wilkerson, 2000; Rowan and Linares, 2000; Wilkerson et al., 2002). In other 2-D studies (e.g. Eisenstadt and DePaor, 1987; Morely, 1994; Woodward, 1997), another level of complexity in kinematics is suggested such that fault-related folds develop with progressive changes in deformation mechanisms. That is, final fold geometry may reflect a composite of several fold mechanisms and fold styles through time.

Based on this previous work and observations from the Rosario seismic data, we propose to further broaden the use of self-similarity as it pertains to 3-D fault-related fold development. Specifically, we suggest a less rigid application of the space-for-time substitution where variables other than displacement are permitted to change along strike, including: changes in fault dip, initial folding followed by thrusting, forelimb dip that increases with time, and later development of active upper and lower detachment horizons. We suggest that the above modifications in fold mechanisms and style through time are consistent with the idea that structures near thrust tips represent early stages of deformation, and those near the crest represent the late stages.

Data do not exist to prove the self-similar model at the Rosario structure. However, the available seismic and well data is consistent with our interpretation of the Rosario structure. Other issues such as the interaction and linkage of multiple faults and the influence of pre-existing basement structures not resolvable with the seismic data could complicate the interpretation. Until better quality data improve imaging of the deeper section at Rosario, we favor the simplest interpretation with the available data and suggest that substituting space for time is a reasonable hypothesis.

3.2. Kinematic model for the Rosario structure

At the crest of the Rosario structure, interpretation of seismic line CCT-90c-14 (Fig. 3d) suggests that the present-day geometry is similar to a fault-bend fold. We interpret on that section that a thrust fault cuts through Cretaceous carbonates and flattens into an upper detachment at the base of the Colon Shale, placing a hanging-wall ramp onto a footwall flat. Similarly, the backlimb appears to return to sub-horizontal, suggesting that the fault soles into a lower detachment. Near the southern termination, however, direct evidence for upper and lower detachments diminishes (Fig. 3g–i). Interpretation of seismic profiles through this area suggests little to no forelimb (if it is present, it seems to have a shallower dip than at the crest; Fig. 4b), an indistinct backlimb, and a fault ramp that emerges from the carbonate section (Fig. 3g–i). Based on this interpretation, the fault changes laterally from fault-bend fold geometry to fault-propagation fold geometry (Fig. 7). Although there is no direct evidence for an active lower flat near the termination (i.e. fold backlimb-to-flat transition), one could be present in order to accommodate the shortening and transfer of displacement to the Rosario East structure. These observations suggest 3-D fault-related fold kinematics that include variations in fold style as well as displacement along strike.

Our model for the evolution of the Rosario structure is shown in Fig. 8. We base this model on the variation in the observed geometry from the crest to the southern termination described above and on the assumption that this spatial variation also represents the temporal variation of the fold since its inception. We do not interpret data below seismically-imaged depths (about 4 s twt), but we recognize that deeper structure might exert some influence on the geometry of the Rosario fault-related fold as it does elsewhere in the basin (e.g. Roure et al., 1997).

During Stage 1 (pre-Mid-Miocene; Fig. 8a), Cretaceous and younger strata are essentially undeformed. Regional uplift and erosion occurred within the western Maracaibo Basin in the Eocene, but no local fold developed at Rosario during this time. During Stage 2 (Mid-Miocene; Fig. 8b), shortening of the section initiates with small reverse offset near the top of the Cretaceous carbonates. This shortening must sole into a proto-lower flat, otherwise the 'basement' or pre-Cretaceous section would be required to shorten. Folding of the overlying Colon Shale occurs simultaneous with fault propagation through the 'stiff' interval of the La Luna and Rio Negro Formations. Sub-seismic scale deformation of the shallow Tertiary clastic section at this time probably is manifested as layer-parallel shortening

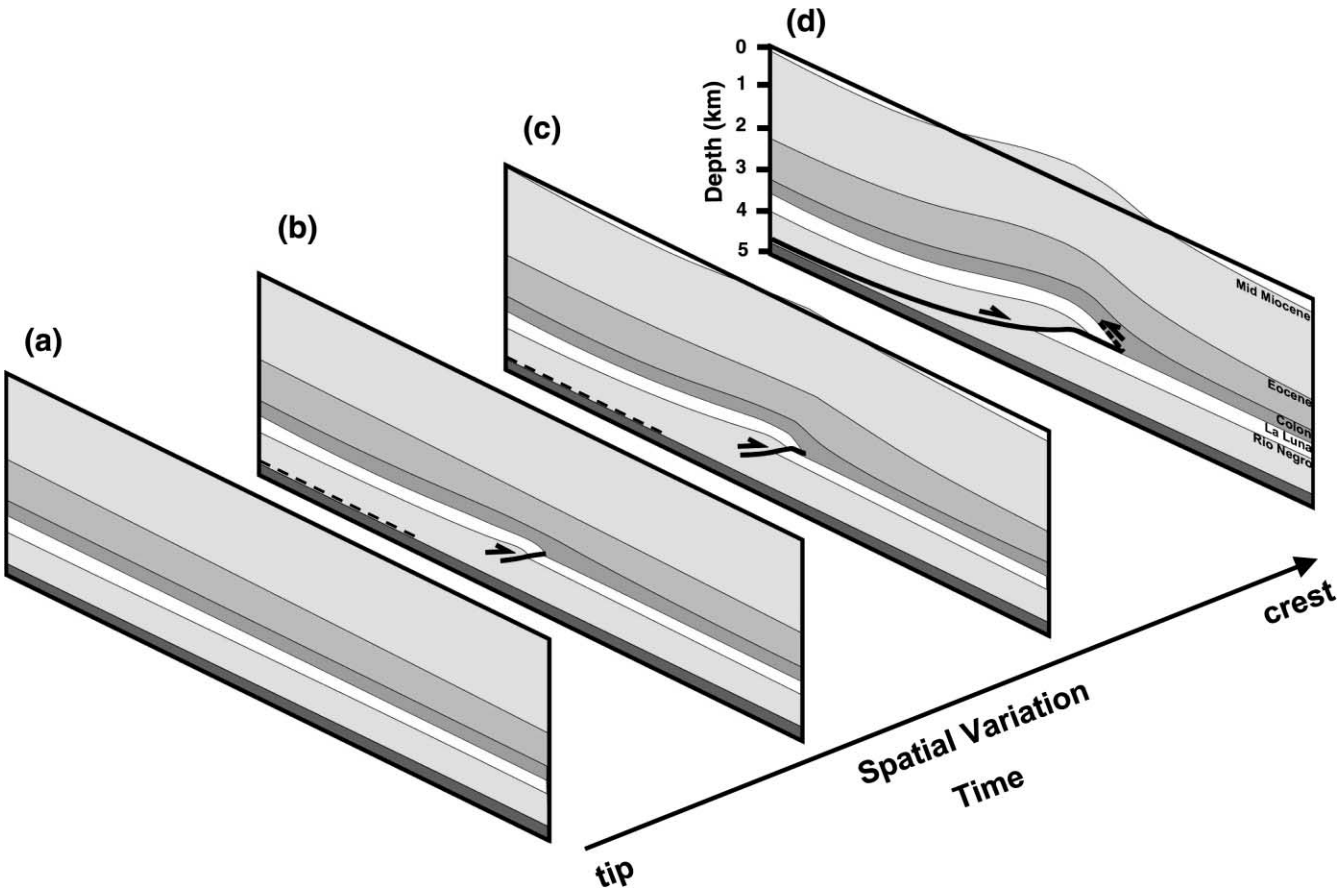

Fig. 8. Model for the 3-D development of the Rosario structure. Each profile represents stages in both the temporal and spatial evolution of the structure from (a) earliest/least displacement to (d) latest/most displacement. In this model, profiles (a) and (b), which resemble the present tip of the Rosario structure (e.g. Fig. 3i), later evolve into profile (d), which resembles the geometry at the present crest of the Rosario structure. See text for more detailed explanation.

(deformation from below most likely was buffered by the thick Colon Shale). At this stage, displacement on the Rosario Fault is so small that no evidence for a backlimb is observed (e.g. Fig. 3g and h). During Stage 3 (Fig. 8c), the fault ramp connects with an upper detachment forming in the Colon Shale. The increased displacement places the hanging-wall ramp onto this upper flat and the forelimb begins to steepen. This is a departure from fault-bend and fault-propagation fold models in which forelimb dip is primarily a function of ramp dip (e.g. Suppe, 1983; Suppe and Medwedeff, 1990), but is supported by the decrease in forelimb dip toward the present-day terminations (see Fig. 4b). Deformation is partitioned by brittle deformation (faulting) and by macroscopically ductile deformation (folding and thickening of the Colon Shale and overlying units). In Stage 4 (Fig. 8d), as displacement accrues, the Rosario fault continues to propagate downward and eventually connects to the basal flat within the Rio Negro or La Quinta Formations. This produces a discrete backlimb-lower flat transition that is observed at the present-day fold crest (and not near the present-day southern termination). Subsequent deformation produces additional fault displacement, which is accommodated primarily by fault-bend folding.

This evolutionary model contains elements of several existing models for fault-related folding. We propose that initially a fault ramp nucleates in stiff carbonates and clastics with associated tip strains accommodated by folding. This interpretation is consistent with a model proposed by Eisenstadt and DePaor (1987) in which a thrust ramp nucleates first and eventually connects with upper and lower detachments. We then suggest that a fault-propagation fold develops as the upper tip propagates, but that fold shape is not exclusively controlled by fault shape. Tip strains and local thickening of the Colon Shale, rather than transfer of displacement out of the structure via the upper detachment, accommodates fault displacement. This stage is consistent with elements of fault-arrest folding (Thorbjornsen and Dunne, 1997) or displacement-gradient folding (Wickham, 1995), in that movement of the upper tip is limited to the Colon Shale, which deforms by local structural thickening similar to the outcrop analog (Fig. 6). In later stages, we propose that the ramp connects to upper and lower detachments, and folding proceeds by modified fault-bend folding. Displacement probably is not transferred into the foreland, but rather is wedged hinterlandward along the base of the Colon Shale. Lastly, as contraction continues, hybridized fault-bend folding accommodates further deformation.

4. Conclusions

The southern termination of the Rosario structure in the western Maracaibo Basin, Venezuela serves as a natural, seismically-constrained example of a contractional fault-related fold termination that forms due to an along-strike decrease in displacement. In addition to the decrease in displacement, other key elements of the interpretation include:

- changes in fault geometry from flat–ramp–flat at the crest of the structure to a fault ramp near the southern tip of the structure,
- a decrease in forelimb dip towards the southern termination, and
- an indistinct backlimb towards the southern termination.

Based on this interpretation, and the assumption that structures at terminations reflect early development of structures in more central portions of fault-related folds, we propose a model for the kinematic development of the Rosario structure. Specifically, we suggest that the structure initially developed as a simple fault ramp with minor folding at its tips (presently observed at Rosario's southern termination), which later propagated to connect with upper and lower detachments. Once connected, the flat–ramp–flat fault geometry produced folding similar to a fault-bend fold (presently observed at Rosario's crest). If our proposed model is correct, then Rosario provides a natural example of a structure where spatial differences reflect temporal stages in the lateral evolutionary development of a fault-related fold. More importantly, it departs from previous models of rigid self-similarity in folding style and permits variations in fold style and deformation mechanisms influenced by mechanical stratigraphy.

Acknowledgements

We wish to acknowledge several ExxonMobil colleagues who contributed discussions pertinent to this work including Jim DeGraff, Michael Kozar, Will Maze, Peter Vrolijk, Barbara Faulkner, Steve Knewtson, Malcom Young, Cliff Ando, Tom Hauge, Rich Wiener, Gary Stone, Clinton Flynn, and Wendel Hoppe. We would also like to thank PDVSA colleagues Isabel Serrano, Nelson Gonzales, Jose Figuera, and Hans Krause. We thank ExxonMobil Upstream Research Company, ExxonMobil Exploration Company, and PDVSA (Venezuela) for permission to publish this work. We used Paradigm Geophysical's Geosec™ for 2-D section construction and depth conversion, and Midland Valley's 3D Move™ for 3-D model building. Acknowledgment is made to the Donors of the Petroleum Research Fund, administered by the American Chemical Society, for support of this research by Wilkerson (specific funding was provided by PRF Grant #33471-GB2). Constructive reviews by Gloria Eisenstadt, Brent Couzens-Shultz, and Mark Fischer are much appreciated. Ted thanks Amy Ruf for advice and editorial support.

References

DeToni, B., Kellogg, J.N., 1993. Seismic evidence of blind thrusting of the northwestern flank of the Venezuelan Andes. Tectonics 12, 1393–1409.

Eisenstadt, G., DePaor, D.G., 1987. Alternative model of thrust fault propagation. Geology 15, 630–633.

Fischer, M.P., Woodward, N.B., 1992. The geometric evolution of foreland thrust systems. In: McClay, K.R. (Ed.). Thrust Tectonics. Chapman & Hall, London, pp. 181–189.

Fischer, M.P., Wilkerson, M.S., 2000. Predicting the orientation of joints from fold shape: results of pseudo-three-dimensional modeling and curvature analysis. Geology 28, 15–18.

Fischer, M.P., Woodward, N.B., Mitchell, M.M., 1992. The kinematics of break-thrust folds. Journal of Structural Geology 14, 451–460.

Hedberg, H.D., 1931. Cretaceous limestones as petroleum source rocks in northwestern Venezuela. American Association of Petroleum Geologists Bulletin 15, 229–244.

Jamison, W.R., 1987. Geometric analysis of fold development in overthrust terranes. Journal of Structural Geology 9, 207–219.

Kellogg, J.N., 1984. Cenozoic tectonic history of the Sierra de Perija, Venezuela–Colombia, and adjacent basins. In: Bonini, W.E., Hargraves, R.B., Shagum, R. (Eds.), The Caribbean–South American Plate Boundary and Regional Tectonics, Geological Society of America Memoir, 162, pp. 239–261.

Maze, W.B. 1984. Jurassic La Quinta Formation in the Sierra de Perija, northwestern Venezuela; geology and tectonic environment of red beds and volcanic rocks. In: Bonini, W.E., Hargraves, R.B., Shagum, R. (Eds.), The Caribbean–South American Plate Boundary and Regional Tectonics, Geological Society of America Memoir, 162, pp. 263–282.

Molina, A., 1992. Rosario Field, Venezuela, Maracaibo Basin, Zulia State. In: Foster, N.H., Beaumont, E.A. (Eds.). American Association of Petroleum Geologists Treatise of Petroleum Geology, Atlas of Oil and Gas Fields, Structural Traps VI. , pp. 293–304.

Morely, C.K., 1994. Fold-generated imbricates: examples from the Caledonides of Southern Norway. Journal of Structural Geology 16, 619–631.

Roure, F., Colletta, B., DeToni, B., Loureiro, D., Passalacqua, H., Gou, Y., 1997. Within-plate deformations in the Maracaibo and East Zulia Basins, Western Venezuela. Marine and Petroleum Geology 14, 139–163.

Rowan, M.G., Linares, R., 2000. Fold-evolution matrices and axial-surface analysis of fault-bend folds: application to the Medina Anticline, Eastern Cordillera, Colombia. American Association of Petroleum Geologists Bulletin 84, 741–764.

Shaw, J.H., Hook, S.C., Suppe, J., 1994. Structural trend analysis by axial-surface mapping. American Association of Petroleum Geologists Bulletin 78, 700–721.

Suppe, J., 1983. The geometry and kinematics of fault-bend folding. American Journal of Science 283, 684–721.

Suppe, J., Medwedeff, D.A., 1990. Geometry and kinematics of fault-propagation folding. Eclogae Geolicae Helvatiae 83, 409–454.

Thorbjornsen, K.L., Dunne, W.M., 1997. Origin of a thrust-related fold: geometric vs. kinematic tests. Journal of Structural Geology 19, 303–319.

Wickham, J., 1995. Fault displacement-gradient folds and the structure at Lost Hills, California (USA). Journal of Structural Geology 17, 1293–1302.

Wilkerson, M.S., 1992. Differential transport and continuity of thrust sheets. Journal of Structural Geology 14, 749–751.

Wilkerson, M.S., Medwedeff, D.A., Marshak, S., 1991. Geometrical

modeling of fault-related folds: a pseudo-three-dimensional approach. Journal of Structural Geology 13, 801–812.

Wilkerson, M.S., Apotria, T.G., Farid, T., 2002. Interpreting the geologic map expression of contractional fault-related fold terminations: lateral/oblique ramps versus displacement gradients. Journal of Structural Geology 24, 593–608.

Woodward, N.B., 1997. Low-amplitude evolution of break-thrust folding. Journal of Structural Geology 19, 293–301.